IL NUOVO CIMENTO **45 C** (2022) 155
DOI 10.1393/ncc/i2022-22155-y

Communications: SIF Congress 2021

Mitigation of non-axisymmetric optical aberrations in Advanced Virgo

C. Taranto(1)(2)(3), E. Cesarini(3), M. Cifaldi(2)(3), V. Fafone(2)(3), M. Lorenzini(2)(3), D. Lumaca(2)(3), Y. Minenkov(3), I. Nardecchia(3) and A. Rocchi(3)

(1) *Department of Physics, University of Rome Sapienza - Rome, Italy*
(2) *Department of Physics, University of Rome Tor Vergata - Rome, Italy*
(3) *INFN, Section of Rome Tor Vergata - Rome, Italy*

received 15 February 2022

Summary. — The sensitivity and operation of ground-based gravitational wave interferometers are limited by noises and optical aberrations. The absorption of power by the mirrors induces their thermal expansion and an increase of the optical path of the light. These effects cause a variation of the nominal optical configuration of the interferometer, worsening its performances. To mitigate these distortions, a thermal compensation system (TCS) has been implemented in Advanced Virgo. TCS is designed to correct two kinds of optical aberrations: the axisymmetric, already tackled, and non-axisymmetric ones. In view of the future observational run, an adaptive control of non-axisymmetric optical aberrations will be needed. The use of Deformable Mirrors (DM) has been studied as a possible solution.

1. – Advanced Virgo

Virgo is the interferometric ground-based detector, founded by INFN and CNRS, located in Cascina, near Pisa, Italy, on the site of the European Gravitational Observatory (EGO). Virgo is one of four large detectors together with the other twin experiments, the LIGO interferometers, located in the United States (one in Hanford and one in Livingston), and with KAGRA, located in Kamioka site (Japan). The Virgo first science run (VSR1) lasted from May to September 2007. Three other science runs have followed. After the conclusion of the VSR4 (Jun 3rd–Sept 5th, 2011), Virgo was turned off in order to start the installation of its upgraded version: Advanced Virgo (AdV) [1]. During the three observing runs (O1, O2 and O3) performed so far, about 90 gravitational wave signals have been detected [2-5]. AdV started joint observation with LIGO in O2. The increase of the number of detections follows the improvements in the detectors' sensitivity. A further improvement is expected in view of O4. The sensitivity curve is given by the sum in quadrature of all noises affecting the detector. In particular, in the high frequency range, the shot noise represents the dominant contribution. It is the effect of the quantum nature of light in reading the signal and it can be reduced either through squeezing techniques [6, 7] as done in O3 or by increasing the injected power. In fact, in the future observational run O5, planned to start in 2025, the input power will be raised by a factor of two with respect to O4 and it will be between 60 and 80 W. So, the power circulating in the Fabry-Perot cavities will be more than 0.5 MW. A fraction (about 0.5 ppm) of the power stored in the arms is absorbed by the Fabry-Perot cavity mirrors, made of fused silica, which means a few hundreds of mW.

2. – Thermal effects and thermal compensation system

Due to poor thermal conductivity of fused silica, even the absorption of the small amount of power in the optics causes a local increase of temperature. Consequently, two effects [8] can arise, the *thermo-optic effect*, due to the variation of local refractive index when the temperature changes, which induces a thermal lens in the bulk, and the *thermo-elastic deformation*, due to the thermal expansion of the materials, responsible for the change in the profile of the high reflectivity surface of the mirror, thus modifying its radius of curvature. A system to correct these distortions is needed. The adopted strategy to compensate the thermal effects is to introduce a complementary distortion restoring the interferometer optimum performance. This is the basis of the *Thermal Compensation System* (TCS) [9]. The correction provided by the TCS concerns the thermal lensing, the thermo-elastic deformation and the correction of defects introduced by the optics manufacturing process (such as inhomogeneities in the refractive index of the bulk or in the absorption of the coating). The thermal compensation system has two actuators: a *Ring Heater* (RH) and a projector based on a *CO_2 Laser*. The Ring Heater is positioned around the test-mass and acts to correct errors in the radius of curvature of the mirrors, either due to thermal effects or to fabrication imperfections. The CO_2 laser projectors are installed on optical benches and the beam is injected in the interferometer through a Zinc Selenide viewport, which is transparent to CO_2 radiation. The CO_2 laser projectors are used to compensate the optical path length distortions due to the thermal lensing generated by the main laser beam in the input test mass substrates or inhomogeneities in the substrate refractive index, due to the fabrication process. CO_2 lasers emit radiation at $\lambda = 10.6\ \mu$m that is completely absorbed by the fused silica. The laser is not directly projected on the mirrors but on an additional transmissive optic, called *Compensation Plate* (CP). CPs are installed in the Anti-Reflective side of the Input Test Masses. The CO_2 laser beam can heat the CP in two different actuation schemes: the *Central Heating* (CH), an axisymmetric centered pattern and the *Double Axicon System* (DAS), an axisymmetric annular correction.

3. – Deformable mirror

The optical aberrations that the TCS system has to correct can be divided into two kinds: the axisymmetric and the non-axisymmetric ones. Regarding the latter, a possible solution, suggested in [8], implies the use of a laser scanning system. This actuation method introduces noise due to the scanner repetition which occurs at a frequency of a few Hz and its harmonics [10]. In order to avoid this issue, deformable mirrors (DM) have been studied as possible future actuators [11]. The great advantage of these systems is that they do not need any beam scanning the mirror surface, so they minimize the noise introduced in the detector. Unlike the typical use in adaptive optics for astronomy, here the DMs are used to apply a phase imprint on the impinging laser beam to obtain the desired intensity pattern at a given plane, needed to correct optical aberrations. The required surface deformation is achieved through actuators located below the DM surface. In the following, the preliminary results of the characterization of a deformable mirror produced by ALPAO [12] are reported. It is made of 97 magnetic actuators with a pupil diameter of 13 mm. The characterization was performed using a green laser with a wavelength of 532 nm.

4. – DM characterization and actuation performances

The characterization has been performed in the Virgo laboratories of the University of Rome Tor Vergata and it has been done using a Shack-Hartmann (SH) wavefront sensor, looking at the phase variation generated by the engagement of each actuator with respect to the flat condition. To compute the actuation vector to be sent to the DM in order to obtain a required deformation, for each actuator a specific quantity has been evaluated, the *influence function*, which is the phase deformation obtained by acting on that single actuator [13]. The influence function of each actuator combines linearly with the ones of all the others giving the surface displacement. The final matrix $\mathcal{A}$, formed by all the elements A_{ij}, is the *influence function matrix*. The influence function of each actuator has been acquired both when raising and lowering the actuators itself and it is obtained by the difference between the wavefront with the actuator engaged and that in flat condition. For each actuator, the raising and lowering influence functions have been taken twice and then averaged. With the measured influence functions, elements A_{ij} have been computed and then influence function matrix $\mathcal{A}$ has been evaluated.

The application of a specific pattern, converted to a vector b, to the DM is obtained by solving $\mathcal{A} \cdot x = b$, where x is the column vector of the actuation coefficients for the reconstruction of the pattern. The inverse matrix $\mathcal{A}^+$ has been calculated by using the *Moore-Penrose pseudoinverse matrix method* [14] and it allows solving the equation in an approximate way as [15] $x = \mathcal{A}^+ \cdot b$, where x is a solution in the least-square sense, *i.e.*, that minimizes the quantity $||\mathcal{A}x - b||_2^2$. The obtained coefficients have been rescaled to DM range. In fig. 1 a first application is shown, where the desired target is a Gaussian pattern. The Root Mean Square of the difference between the target and the reconstructed target is 7.7 nm and the RMS of the difference between the reconstructed target and the experimental one is 12.5 nm. The DM is able to reproduce the desired target within an error of 1%.

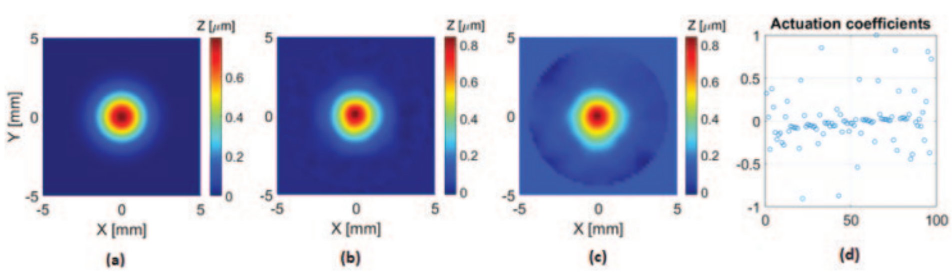

Fig. 1. – Evaluation of the actuation coefficients with the pseudoinverse matrix. After choosing a pattern as a target (a), the actuation coefficients are computed (d) and from them the expected pattern (b) can be simulated to be compared with the experimental result (c).

5. – Conclusions

A deformable mirror has been characterized by performing the evaluation of the influence functions of all its actuators and by building the influence function matrix. A good reconstruction of the chosen target profiles is obtained in the case of a simple profile. As next steps, the capability of the DM to reproduce more complex profiles like those needed for AdV will be investigated, and the optical simulations to assess the quality of compensation necessary to correct the non-axisymmetric optical aberrations inside the interferometer will be performed. Another important step to take, which has already started, is the investigation of the phase retrieval algorithms, since the mirror maps to be corrected are in terms of intensity, but the DM response is only a phase actuation. In this way, full characterization with a CO_2 laser, like those used in Advanced Virgo, will be performed.

REFERENCES

[1] Acernese F. *et al.*, *Class. Quantum Grav.*, **32** (2015) 024001.
[2] LIGO Scientific Collaboration and Virgo Collaboration, *Phys. Rev. X*, **9** (2019) 031040.
[3] LIGO Scientific Collaboration and Virgo Collaboration, *Phys. Rev. X*, **11** (2021) 021053.
[4] LIGO Scientific Collaboration, Virgo Collaboration and KARGA Collaboration, *GWTC-3: Compact Binary Coalescences Observed by LIGO and Virgo During the Second Part of the Third Observing Run,* arXiv:2111.03606 [gr-qc] (2021).
[5] LIGO Scientific Collaboration and Virgo Collaboration, *Astrophys. J. Lett.*, **915** (2021) 1.
[6] Virgo Collaboration, *Phys. Rev. Lett.*, **123** (2019) 231108.
[7] Virgo Collaboration, *Phys. Rev. Lett.*, **125** (2020) 131101.
[8] Lawrence C. R., *Active Wavefront Correction in Laser Interferometric Gravitational Wave Detectors*, PhD Thesis (MIT, USA) 2003.
[9] Rocchi A., Coccia E., Fafone V., Malvezzi V., Minenkov Y. and Sperandio L., *J. Phys.: Conf. Ser.*, **363** (2012) 012016.
[10] Lorenzini M. and Puppo P., *Effect of the CO_2 scanning system on CP motion*, Virgo internal note VIR-0574A-13 (2013).
[11] Rocchi A., *Thermal effects and other wavefront aberrations in recycling cavities, Advanced Interferometers and the Search for Gravitational Waves, Lectures from the First VESF School on Advanced Detectors for Gravitational Waves*, edited by Bassan M. (Springer) 2014.
[12] `https://www.alpao.com/`.
[13] Clain E. S. and Bareket N., *J. Opt. Soc. Am. A*, **3** (1986) 1833.
[14] Penrose R., *Proc. Cambridge Philos. Soc.*, **51** (1955) 406.
[15] James M., *Math. Gazette*, **62** (1978) 109.